CHAPTER 1

# The multiscale nature of the brain and traumatic brain injury

**M.A. Murphy**[a], **A. Vo**[a,b]

[a]*Center for Advanced Vehicular Systems (CAVS), Mississippi State University, Mississippi State, MS, United States* [b]*Department of Agricultural and Biological Engineering, Mississippi State University, Mississippi State, MS, United States*

## 1.1 Introduction

The human brain is a truly amazing structure that is complex both in its function and its anatomical multiscale hierarchy. While other organs and systems in the human body also exhibit unique and complex multiscale geometrical hierarchies, the brain's anatomical, physiological, and mechanical properties provide a very difficult problem for consideration. Scientists are still working to understand the brain's "normal" physiological responses and structures, and changes due to injuries can be even more confounding.

Generally, injuries to the brain are broadly classified under the term traumatic brain injury, which is commonly abbreviated as TBI. These injuries are one of the leading causes of mortality and disability globally (Humphreys et al., 2013; Taylor et al., 2017) and primarily due to accidents from sports and motor vehicles (Andriessen et al., 2010; Johnson et al., 2013). These and other injury events cause external mechanical forces to the head that can cause physical damage and dysfunctionality to the brain.

The question of what TBI is has been discussed and changed many times, including the initial distinction from the general classification of head injury (Menon et al., 2010). As a general definition, "TBI is defined as an alteration in brain function, or other evidence of brain pathology, caused by an external force" (Menon et al., 2010). In other words, TBI is any acceleration or impact that affects brain function or pathology.

While this description is very broad, TBI can be identified through observing an individual that has potentially sustained injury. A common way to identify an alteration in the brain's function is by observing apparent changes in an individual's mental or physical condition, such as loss of consciousness, memory loss, neurological deficits (weakness or sensory loss), or mental state alterations (confusion) (Menon et al., 2010). These changes can be short-lived or endure over longer periods of time. Alternatively, brain pathology can be viewed clinically using medical imaging, such as magnetic resonance imaging (MRI) or diffuse tensor imaging

**Multiscale Biomechanical Modeling of the Brain.**
**DOI: https://doi.org/10.1016/B978-0-12-818144-7.00004-9**

(DTI) (Menon et al., 2010; Sabet et al., 2008). However, these images do not give information about the state of the brain during the process of injury, only the aftereffects of the injury. This limitation results in knowledge gaps regarding the injury process. Further, they may not allow an injury to be observed if it is not severe enough.

Mechanically speaking, when the head is subjected to a rapid acceleration or deceleration, TBI can result due to local strains within the brain, leading to various issues, including neuronal bilayer membrane deformation leading to mechanoporation, water molecule penetration, and the rearrangement of phospholipids (Prabhu et al., 2011; Murphy et al., 2016, 2018). This deformation causes membrane disruption and alters ion flow across the membrane, which can have a significant impact on the membrane's structural and dynamic properties as well as affect the transmembrane potential and cellular homeostasis (Murphy et al., 2018; Alaei, 2017). Eventually, these events can induce cell death, tissue damage, and brain dysfunction at higher length scales. Nonetheless, those cellular impairments, unlike visible macroscale structural and functional damages (e.g., bruises, bleeding, lacerations, etc.), are often too subtle to be detected or quantified in real-time studies through current imaging techniques or in vivo and in vitro measurements (Alaei, 2017; Montanino, 2019). These approaches are hindered by the time and spatial resolution as well as the seeming mismatch between cellular and subcellular scale physiological changes and damage observations at the organ scale (Murphy et al., 2018; Montanino, 2019; Rashid et al., 2013, 2014).

Determining each length scale's effect on the brain's mechanical properties and resulting pathology is of utmost importance because each can have profound effects on the macroscale brain's response. However, the multiscale nature of the brain and its injury mechanisms as well as the inability to easily observe injury mechanisms in real time can make this task unmanageable very quickly. Instead, each length scale must be considered separately to determine which boundary conditions must be scaled down from higher length scales and what information must be passed up from lower length scales. A graphical representation of this process is shown in Fig. 1.1. Then, experiments and simulation methods can be used to examine TBI at the length scale where each injury mechanism occurs.

## 1.2 The brain's multiscale structure

As mentioned above, the human brain has complex anatomical (geometrical) hierarchy. While the brain's complexity does make it more difficult to understand, being multiscale is not unique to the brain or even biological structures. Typically, any material or structure with properties from multiple length scales that can affect the overall properties can be described as multiscale, which necessitates that lower length scales be considered when considering mechanical responses and damage. Biological structures, like the brain, are often vastly different at the different length scales. For example, tendons have six distinct structural scales (tendon, fascicle, fiber, fibril, subfibril, and tropocollagen), which spans from the nanometer

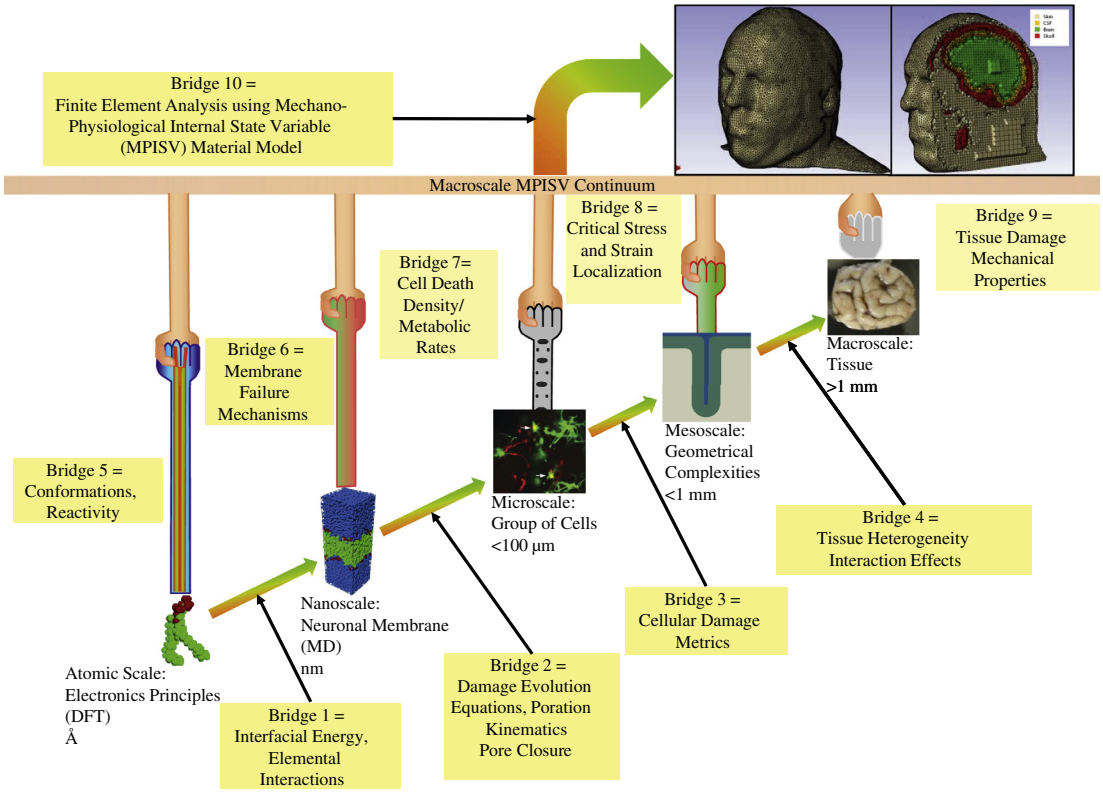


**Fig. 1.1: Multiscale structure of the brain that will be used for the modeling and simulation discussed in the later chapters of this book.**

to millimeter length scales (Harvey et al., 2009). For the brain, this complex multiscale structural hierarchy includes the brain, lobes, regions, sulci and gyri, groups of cells, individual cells, cellular organelles, and components. Therefore, a broad overview of the brain's multiscale anatomy has been included here.

### *1.2.1 Gross anatomy*

The brain is covered with connective tissues that make up a system of membranes called meninges, which include the outer dura mater, the middle arachnoid mater, and the inner pia mater (Purves, 2012; Snell, 2010). Dura mater is a strong, thick, and nonelastic membrane that folds into septa, including the falx cerebri that separates the right and left half of the brain (Montanino, 2019; Kekere and Alsayouri, 2019). Arachnoid mater is a thin, web-like membrane that stretches between the dura and pia mater. Pia mater is another thin layer that tightly wraps the entire surface of the brain and aids in the production of cerebrospinal fluid (Patel and Kirmi, 2009; Decimo et al., 2012). The cerebrospinal fluid acts as a cushion in these protective layers, helping the brain preserve its shape and anchoring it in place within the

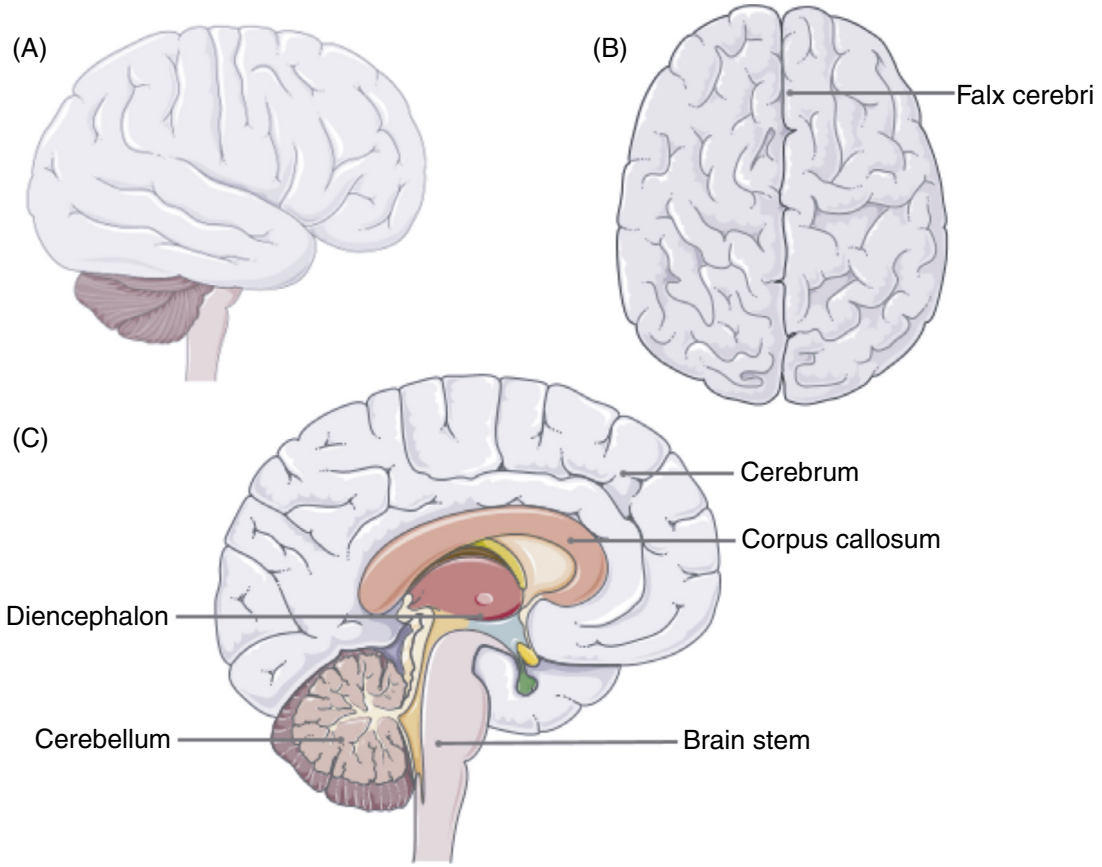


**Fig. 1.2: Representative schematics of the brain (A) side and (B) top views and (C) brain structures. Images are modified and used with permission from Servier Medical Art - Creative Commons Attribution 3.0 Unported License.**

skull (Patel and Kirmi, 2009; Decimo et al., 2012). If the brain is viewed in three dimensions and the meninges are removed, it contains four main divisions called cerebrum, cerebellum, brainstem, and diencephalon (Patestas and Gartner, 2016). The cerebrum, the cerebellum, and the brainstem are clearly visible, while the diencephalon is almost completely hidden from the brain surface (Snell, 2010; Patestas and Gartner, 2016) (Fig. 1.2).

#### *1.2.1.1 Cerebrum*

The cerebrum consists of two nearly symmetrical hemispheres and is covered by the cerebral cortex, which is 2–4 mm and highly folded (Patestas and Gartner, 2016; Kandel et al., 2000). Each fold or ridge is called a gyrus, and each groove between the folds is called a sulcus. Some large sulci are named according to their position or also called fissure, which divide the cerebrum into different regions (Snell, 2010; Patestas and Gartner, 2016; Squire et al., 2013). The cerebrum is incompletely separated into left and right hemispheres by a deep longitudinal

fissure containing the falx cerebri, and joined again by the corpus callosum at the end of that fissure (Patestas and Gartner, 2016; Davey, 2011). Shown in Fig. 1.3, each hemisphere is subdivided into four main broad regions or lobes: the frontal, parietal, temporal, and occipital lobes (Snell, 2010; Patestas and Gartner, 2016; Gray and Standring, 2015). Besides, there are limbic and insular lobe (insula) hidden inside the hemisphere (Patestas and Gartner, 2016; Squire et al., 2013). The frontal lobe is the primary motor area, controlling movement, behaviors and personality, attention, and concentration (Snell, 2010; Patestas and Gartner, 2016; Kolb and Whishaw, 2009). The parietal lobe is the primary somesthetic area that integrates somatosensory information. The temporal lobe is the major processing center of auditory information (Patestas and Gartner, 2016; Freberg, 2009). The occipital lobe is the smallest lobe whose main functions are visual-spatial processing (Snell, 2010; Patestas and Gartner, 2016). The insula is associated with taste, visceral sensation and autonomic control (Patestas and Gartner, 2016). The limbic lobe is the cortical constituents of the limbic system, which is the center of emotions, learning and memory (Patestas and Gartner, 2016). Each lobe could be further divided into smaller regions serving very specific functions, making up approximately 50 functional areas in the cortex (Guyton and Hall, 2011).

Besides being divided into regions, the cerebral cortex is also organized in layers, which are characterized by different densities, sizes and morphology of 16 billion nerve cells or neurons (Bastiani and Roebroeck, 2015; Bigos et al., 2016; Azevedo et al., 2009). The cortex is classified into archicortex (allocortex), mesocortex (juxtallocortex), and neocortex (isocortex) (Patestas and Gartner, 2016). The archicortex contains three layers and is situated at the limbic system, while the mesocortex has three to six layers and is predominant in the insula and above the corpus callosum. The neocortex consists of six layers, which is known as the cytoarchitecture and comprises the bulk of the cerebral cortex (Patestas and Gartner, 2016; Bastiani and Roebroeck, 2015). Passing through this cytoarchitecture are cell columns, each of which is less

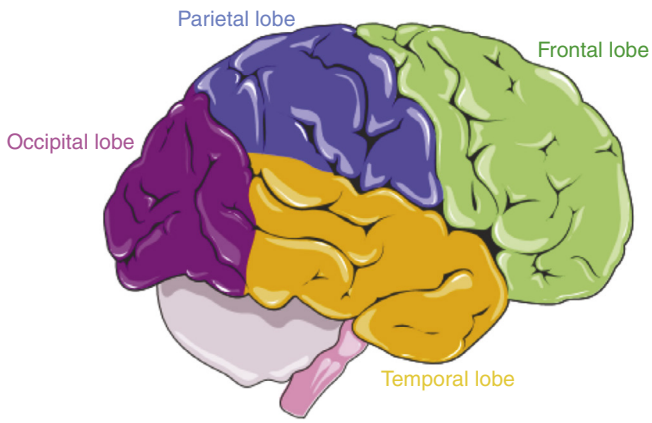


**Fig. 1.3: Main lobes of the brain. Images are modified and used with permission from Servier Medical Art - Creative Commons Attribution 3.0 Unported License.**

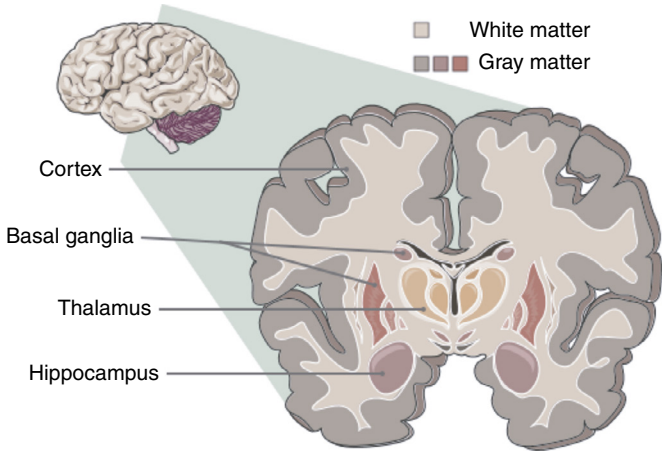


**Fig. 1.4: Schematic representation of a brain section showing gray and white matter. Images are modified and used with permission from Servier Medical Art - Creative Commons Attribution 3.0 Unported License.**

than 0.1 mm wide, perpendicular to the cortical surface and consists of neurons with similar functions (Patestas and Gartner, 2016). The cortical layers are made up of gray matter, which contains soma (nerve cell bodies or nuclei) and can be found at the brain regions involved in controlling muscular and sensory activity (Montanino, 2019). Beneath the cortex, deeper subcortical regions are made up of white matter, which includes axon (nerve fibers), connects different areas of the brain and the brain with other body parts (Patestas and Gartner, 2016; Bastiani and Roebroeck, 2015; Sampaio-Baptista and Johansen-Berg, 2017). Gray matter are also present within the white matter, in the deep structures of the cerebrum, diencephalon, cerebellum, and brainstem, such as the hippocampus, thalamus, hypothalamus, and basal ganglia (basal nuclei) (Montanino, 2019; Snell, 2010). A representative view of these structures shown in Fig. 1.4. Within the cerebrum, the basal ganglia acts alongside the cerebral cortex as part of the cognitive system (Purves, 2012; Patestas and Gartner, 2016; Stocco et al., 2010). The basal nuclei convey information to various brain regions and work with the cerebellum to control complex muscle movements (Patestas and Gartner, 2016; Guyton and Hall, 2011).

#### *1.2.1.2 Cerebellum*

The cerebellum is located below the cerebrum and consists of two cerebellar hemispheres connected by the narrow vermis (Snell, 2010). The vermis is subdivided into superior and inferior portion, which are respectively visible and hidden between the two hemisphere (Snell, 2010; Patestas and Gartner, 2016). The cerebellum has an outer surface made up of gray matter and an inner core composed of white matter (Patestas and Gartner, 2016; Gray and Standring, 2015). Certain masses of gray matter can also be found in the interior of the cerebellum and embedded in the white matter (Patestas and Gartner, 2016). The surface of the cerebellum is called cerebellar cortex, which is much thinner than the cerebral cortex and

organized in three layers—the outermost molecular layer, the middle Purkinje layer, and the innermost granular layer (Patestas and Gartner, 2016; Gray and Standring, 2015). The cerebellar cortex has slender and parallel folds called folia, alternating with the grooves called sulci (Snell, 2010; Patestas and Gartner, 2016). Some deep sulci or fissures further subdivide each hemisphere into three lobes—anterior, posterior, and flocculonodular lobes (Patestas and Gartner, 2016; Guyton and Hall, 2011). The anterior and posterior lobes are separated by the transverse primary fissure and play an important role in coordinating complex muscle movements. The flocculonodular lobe is underneath these two lobes and is essential in maintaining balance (Patestas and Gartner, 2016; Guyton and Hall, 2011). Although the cerebellum is argued to be involved in some cognitive control, its main function is in motor control, maintenance of posture and balance (Squire et al., 2013; Guyton and Hall, 2011). It is linked to the cerebral motor strip and contributes to the precision of motor activity (Fine et al., 2002). The cerebellum and the basal ganglia, together with the thalamus in the diencephalon, work as the main movement coordination center that fine-tune motor functions.

#### *1.2.1.3 Diencephalon*

Besides the cerebrum and cerebellum, diencephalon is another structure that contains large collections of gray matter. It is hidden from the surface of the brain, interposed between the cerebrum and the brainstem, and is separated in two halves by the third ventricle—a narrow space filled with cerebrospinal fluid (Snell, 2010; Patestas and Gartner, 2016). The diencephalon consists of four components: the epithalamus, thalamus, hypothalamus, and subthalamus (Snell, 2010; Patestas and Gartner, 2016). The epithalamus is the dorsal posterior segment of the diencephalon, linking the limbic system with other parts of the brain (Caputo et al., 1998). It contains the pineal gland that modulates the body's internal clock, circadian rhythms, and sex hormones (Aulinas, 2000; Lowrey and Takahashi, 2000). The hypothalamus is located in the floor of the third ventricle and forms the ventral part of the diencephalon (Snell, 2010). It links the nervous system to the endocrine system through the pituitary gland, which secrets hormones for metabolism, growth and sexual development (Boron and Boulpaep, 2016). Located above the hypothalamus is the thalamus, both of which are part of the limbic system (Boeree, 2009). The thalamus is separated with the hypothalamus by the hypothalamic sulcus situated along the lateral walls of the third ventricle. The right and left thalami constitute the bulk of the diencephalon and are connected by a bridge of gray matter called interthalamic adhesion or massa intermedia. The thalamus functions as a relay station integrating and conveying information to the cortex (Gazzaniga et al., 2014), which is responsible for alertness, sensation and memory (Sherman, 2006; Sherman and Guillery, 2009; Aggleton et al., 2010). At the back of the thalamus is the brainstem (Higgins, 2006).

#### *1.2.1.4 Brainstem*

The brainstem is a stalk-like structure that connects the cerebrum, cerebellum, and diencephalon to the spinal cord (Snell, 2010; Patestas and Gartner, 2016). It is partly hidden

by the cerebrum and cerebellum, linked to the cerebellum by the cerebellar peduncles, and consists of the midbrain, the pons, and the medulla oblongata (Patestas and Gartner, 2016; Gray and Standring, 2015). The brainstem controls the cardiovascular and respiratory system, consciousness, reflexes, and automatic processes (e.g., breathing, eye movements, swallowing, and digestion) (Gray and Standring, 2015; Guyton and Hall, 2011). It consists of many nerve tracts and nerve nuclei of the central as well as peripheral nervous system. Particularly, 10 of the 12 pairs of the nerves of the central nervous system (cranial nerves III through XII) directly emerge from the brainstem (Snell, 2010). Hence, it serves as a channel for transmitting information between the brain and different parts of the body, including the ascending tracts (the nerve pathways carrying sensory information from the body up the spinal cord to the brain) and descending tracts (the nerve pathways carrying motor information from the brain down the spinal cord to the body) (Snell, 2010; Gray and Standring, 2015).

### 1.2.2 Microanatomy

The cerebrum, the cerebellum, the diencephalon, and the brainstem are built from nervous tissues, which can be divided as gray and white matter (Montanino, 2019; Bastiani and Roebroeck, 2015). They are microscopically constituted from an abundance of cells, including two main categories: (1) non-neuronal cells (glia cells or neuroglia) consisting of microglia and macroglia (Montanino, 2019); (2) neuronal cells (nerve cells or neurons) comprising cell body or soma, branching dendrites and a longer projection called axon, in which the axon can be unmyelinated or myelinated (interruptedly wrapped by layers of a plasma membrane named myelin) (Alberts et al., 2014). Gray matter includes cell bodies in gray–brown color, dendrites, some glia cells and unmyelinated neurons (Montanino, 2019; Patestas and Gartner, 2016). White matter is made up of bundles of myelinated neurons, in which the myelin sheath covering the axon gives it the white color (Montanino, 2019; Gray and Standring, 2015). Overall, the human brain contains approximately 85 ± 10 billion of neuroglia and 86 ± 8 billion neurons, in which 16 billion neurons are in the cerebral cortex and 69 billion neurons are in the cerebellum (Bigos et al., 2016; Azevedo et al., 2009). Neurons are the key functional units of the brain, while the neuroglia provide them with nourishment, protection and structural support (Patestas and Gartner, 2016; Squire et al., 2013).

#### 1.2.2.1 Neuroglia

The neuroglia can be divided into microglia and macroglia (Montanino, 2019), representative examples of which are shown in Fig. 1.5. Microglia are scattered throughout the brain and spinal cord (Snell, 2010; Ginhoux et al., 2013). From their cell bodies arise wavy branches or processes that give off multiple spine-like projections (Snell, 2010). They are responsible for the immune response and overall maintenance of the brain, continuously scavenging it for damaged neurons or infectious agents, and protecting it from invaders (Patestas and Gartner, 2016; Helmut et al., 2011). Macroglia consists of astrocytes, oligodendrocytes, and ependymal cells. Astrocytes are the largest neuroglia, consisting of fibrous and protoplasmic

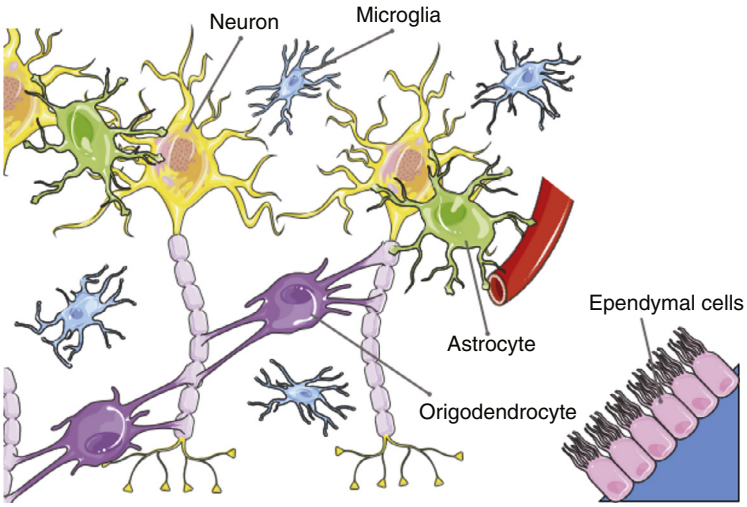


**Fig. 1.5: Pictorial representation of neuroglia and neurons. Images are modified and used with permission from Servier Medical Art - Creative Commons Attribution 3.0 Unported License.**

type, with small cell bodies and branching processes extending in all directions (Snell, 2010). Fibrous astrocytes are present mostly in white matter, where their long, slender and not much branched processes pass between the nerve fibers (Snell, 2010; Patestas and Gartner, 2016). Protoplasmic astrocytes are located mainly in gray matter, where their short, thick and branched processes pass between the nerve cell bodies (Snell, 2010; Patestas and Gartner, 2016). These astrocytes conduct metabolites, regulate blood flow, and form a supporting framework for the neurons (Snell, 2010). They regulate the uptake of neurotransmitters (electrical or chemical substances delivered between neurons), maintain ionic balance and modulate neural activity (Oberheim et al., 2012), as well as take up and replace dead neurons or degenerating axon terminals (Snell, 2010; Patestas and Gartner, 2016). Oligodendrocytes, with small cell bodies and a few delicate processes, are frequently found surrounding nerve cell bodies and along myelinated neurons (Snell, 2010). They can expand their membrane to form myelin sheaths that wrap around and insulate up to 50 axons, allowing electrical messages to travel faster (Saab and Nave, 2017). The third type of macroglia, ependymal cells, forms a single layer of cuboidal cells that line the brain ventricles, circulates cerebrospinal fluid and prevents it from leaking into underlying tissues (Snell, 2010; Patestas and Gartner, 2016). Altogether, the role of these neuroglia, although highly diverse and incompletely understood, is creating an environment where neurons can develop and function (Montanino, 2019; Herculano-Houzel, 2014).

#### *1.2.2.2 Neurons*

Neurons are electrically excitable nerve cells specializing in receiving, transmitting, and conducting electrochemical signals or nerve impulse (Snell, 2010; Patestas and Gartner, 2016).

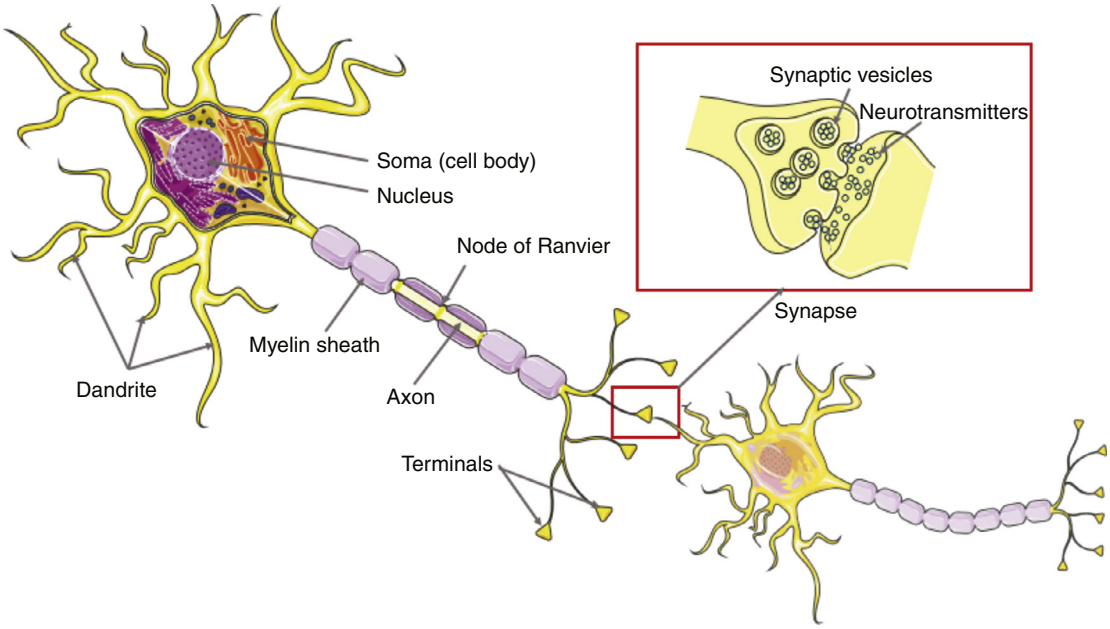


**Fig. 1.6: Pictorial representation of neuron and intercellular communication. Images are modified and used with permission from Servier Medical Art - Creative Commons Attribution 3.0 Unported License.**

A representative neuron is shown in Fig. 1.6. They vary in size, shape, location, connectivity, and neurochemical characteristics, but all have similar structures (Squire et al., 2013). Morphologically, each neuron consists of a cell body (soma or perikaryon) and multiple processes (neurites, composed of dendrites and axon) branching from the cell body, which facilitates intercellular communication through synapses (small gaps between the cells) (Snell, 2010; Patestas and Gartner, 2016; Alberts et al., 2014).

The nerve cell body, similar to other cells, contains a nucleus, cytoplasm and is enclosed by a plasma membrane (Montanino, 2019; Snell, 2010). The cytoplasm is rich in granular (rough) and agranular (smooth) endoplasmic reticulum (ER), which is an interconnected network of flattened, membrane-enclosed sacs (cisternae) that synthesize and transport cellular materials such as proteins, lipids and carbohydrates (Snell, 2010). It contains the nucleus, cytoplasmic organelles (including Nissl substance and Golgi complex), and the cytoskeleton needed for the functioning of the cell (Snell, 2010; Squire et al., 2013). The nucleus is typically rounded, centrally located within the cell body, and has an envelope made from two lipid bilayer membranes. It stores the genes and controls the cell activity (Snell, 2010). The Nissl substance contains stacks of rough ER interposed with ribosomes, distributed throughout the cytoplasm, extended into the proximal parts of the dendrites and absent from axon (Squire et al., 2013). Ribosomes containing RNA and protein are attached to the ER surface or insinuated between the cisterna, enabling the Nissl to synthesize proteins that flow along the

neurites (Snell, 2010; Squire et al., 2013). The protein is then transferred to the Golgi complex in transport vesicles, where it is temporarily stored and maybe added with carbohydrate to form glycoproteins that contribute to the synthesis of cell membranes (Snell, 2010; Squire et al., 2013). The Golgi complex appears around the nucleus as clusters of cisternae made up of smooth ER, modifying and transporting vesicles of macromolecules to the nerve terminals (Snell, 2010).

Another feature of the cytoplasm, which extends throughout the cell body and its processes, is the cytoskeleton. It is composed of microfilaments (actin filaments), neurofilaments (intermediate filaments), and microtubules (Montanino, 2019; Squire et al., 2013). Microfilaments are helical polymers formed of actin (with a diameter of 3–5 nm in soma or 7–9 nm in axon), concentrated at the periphery of the cytoplasm (Snell, 2010; Fletcher and Mullins, 2010). They form a dense network beneath the plasma membrane, assist in cell transport, forming and retracting cell processes (Montanino, 2019; Snell, 2010). Larger than the microfilaments are the neurofilaments (with a diameter of about 10 nm). They are the main components of the cytoskeleton, which bundle together to form parallel neurofibrils running through the cell body into the neurites, determine the shape of neurons and axonal radial growth (Montanino, 2019; Snell, 2010). The biggest and stiffest components of the cytoskeleton are microtubules (hollow cylinders with an outer diameter of 25 nm). They are interspersed among the neurofilaments and composed of 13 protofilaments of tubulin heterodimers that are continuously added or removed at both ends (Snell, 2010; Fletcher and Mullins, 2010). In axons, they form dense bundles with uniform orientation—the fastest growing end pointing toward the axonal tip and the other end pointing to the cell body (Montanino, 2019). These microtubules, together with the microfilaments, provide a stationary track for specific organelles to move by molecular motors (Snell, 2010). On the whole, the filament network has two main roles: maintain the shape of the neuron and allow cellular transport along its structure (Montanino, 2019).

Besides the cytoskeleton, the plasma membrane is another component that extends from the soma into the axon and dendrites. The membrane is about 8 nm thick, mainly composed of lipids and proteins arranged in layers, in which the middle lipid bilayer (about 3 nm) separates the inner and outer layer of loosely arranged proteins (about 2.5 nm each) (Alaei, 2017; Montanino, 2019; Snell, 2010). The lipid bilayer is made up of phospholipids, each with two hydrophobic tails pointing inward and the polar headgroup pointing outward in contact with the protein layers (Alaei, 2017; Snell, 2010). Certain proteins span the entire width of the lipid bilayer, forming hydrophilic channels through which inorganic ions enter and leave the cell (Snell, 2010). Besides lipids and proteins, cholesterols (CHOL) are another important components (Alaei, 2017). Together they determine membrane properties such as stiffness, bending and permeability (Alaei, 2017; Harayama and Riezman, 2018). Additionally, carbohydrate molecules are attached outside the membrane and linked to the proteins or the lipids, forming the cell coat or glycocalyx (Snell, 2010). The plasma membrane and the cell

coat form a semipermeable membrane, allowing diffusion of ions. When the neuron is resting (unstimulated), the passive efflux of $K^+$ (from the cytoplasm to the extracellular fluid) is greater than the influx of $Na^+$ (from the extracellular fluid into the cytoplasm), which makes the inside of the membrane more negative and results in the resting potential between -50 mV and -80 mV (Montanino, 2019; Snell, 2010). When the neuron is excited (simulated), the membrane permeability to $Na^+$ rapidly increases, progressively depolarizing the membrane and producing the action potential of +40 to +50 mV (Montanino, 2019; Snell, 2010). The increased permeability for $Na^+$ quickly stops after 5 milliseconds and the permeability for $K^+$ efflux increases again. The action potential spreads over the membrane and self-propagates along the neurites as nerve impulse (Snell, 2010). In general, the plasma membrane defines the intracellular-extracellular boundary, regulate the transport of materials and signals, and serves as the site for the initiation and conduction of the nerve impulse (Montanino, 2019; Giordano and Kleiven, 2014).

Although neurons resemble other cells in the body, they are distinguished by branching processes or neurites, including dendrites and axon (Montanino, 2019; Patestas and Gartner, 2016). Dendrites are short processes with tapered diameter and cytoplasm similar to the cell body (Snell, 2010). They branch profusely into dendritic shafts, which further protrude several smaller projections (about 2 μm) called dendritic spines (Snell, 2010; Squire et al., 2013). The spines regulate neurochemical events and increase the receptive surface for the cell body (Squire et al., 2013). Dendrites receive electrochemical stimulation or nerve impulse from other neurons via their synaptic terminals, then the inputs are conducted toward the cell body and transmitted along the axon (Montanino, 2019; Snell, 2010; Squire et al., 2013). Axon is a single long tubular neurite at the other pole of the neuron, extending farther from the cell body and containing more filaments than dendrites (Snell, 2010; Squire et al., 2013). Axon is the longest process (about 0.1 mm), with smooth surface and several branches (collaterals) along its length (Snell, 2010; Squire et al., 2013). Axon has a typical cellular architecture, including a cytoplasm (axoplasm) bounded by a plasma membrane (axolemma or plasmalemma). Axoplasm does not contain Nissl substance, Golgi complex, and the sites producing proteins (RNA and ribosomes) (Montanino, 2019; Snell, 2010). Meanwhile, axolemma is similar to the membrane of the cell body, containing ion channels that control the transmembrane ion flux and connect to the axonal cytoskeleton (Alberts et al., 2014; Leterrier et al., 2017). Most axons are surrounded by an insulating myelin sheath—an extended plasma membrane composed of lipoproteins and produced by oligodendrocytes (Montanino, 2019; Squire et al., 2013). Myelinated axonal portions (internodal segments) are interrupted by unmyelinated ones (nodes of Ranvier) clustered with sodium channels (Montanino, 2019). This configuration allows the action potential to propagate by jumping from node to node, facilitating efficient impulse conduction (Montanino, 2019; Squire et al., 2013). The axon leaves the cell body from a small elevated area called axon hillock, then the first 50–100 μm is the axon initial segment (AIS) rich in voltage-gated channels (Alberts et al., 2014; Kole et al., 2008). AIS is the most excitable axonal part, at which the action potential originates

and the stimulation that a neuron receives is encoded for long-distance transmission (Snell, 2010; Alberts et al., 2014). After that the axon emits numerous collaterals with enlarged ends called terminals, forming synapses with other neurons (Montanino, 2019; Snell, 2010). An axon conducts nerve impulses away from the cell body and communicates with other neurons at synapses, where the neurotransmitters are released and bind to receptor molecules on the receiving neuron (Patestas and Gartner, 2016; Squire et al., 2013).

The synapse is a site of neuronal communication, in which an axon of one neuron makes contact with the dendrite or cell body, or rarely with the initial segment or terminals of another axon (Snell, 2010; Squire et al., 2013). Depending on the site of contact, synapses are referred to as axodendritic, axosomatic, or axoaxonic (Snell, 2010). Each synapse consists of a presynaptic element (a portion of the axon making the contact), a narrow synaptic cleft, and a postsynaptic element (a portion of the receiving dendrite, soma, or axon) (Snell, 2010). The portion of the presynaptic element proximate to the postsynaptic element is the active zone, where the synaptic vesicles are concentrated or anchored for fusion. The active zone is enriched with voltage-gated calcium channels that aid in the vesicle fusion and the release of neurotransmitter into the synaptic cleft (Squire et al., 2013). The synaptic cleft is around 20 μm, determining the volume where each synaptic vesicle releases its contents and the maximum concentration of released neurotransmitters (Squire et al., 2013). Several neurotransmitters could be released, one of which is the key activator functioning directly on the postsynaptic membrane, while others modulate its activities (Snell, 2010). The synapses excites or inhibits the neuron when the released neurotransmitters cause a small depolarization (excitatory postsynaptic potential) or hyperpolarization (inhibitory postsynaptic potential) in the postsynaptic membrane (Alberts et al., 2014). Overall, a single neuron receive inputs from thousands of other neurons through neurotransmission, and can form synapses with thousands of other neurons (Snell, 2010; Alberts et al., 2014). This interneuronal communication forms tree-like structures called neuronal arbors, which are responsible for distributing information over a region of the brain (Teeter and Stevens, 2011). Furthermore, the neuronal arbors connect together to form local circuits that constitute the structural and functional basis for the brain activity (Snell, 2010; Squire et al., 2013).

## 1.3 The multiscale nature of TBI

While TBI can be the result of an externally visible injury with a clear cause, such as a puncture wound or blast wave, TBIs often occur due to less apparent causes as well and range in severity from mild to severe. Importantly, injury severity greatly influences both the ability to detect TBI cases as well as a patient's expected short-term and long-term outcomes, which can include death due to injury. To understand this problem better, a broad overview of injury mechanisms at each length scale, injury types and examples, neurobehavioral sequelae, and research methods are explored here.

### 1.3.1 Multiscale injury mechanisms

The brain's multiscale properties also affect how the brain is damaged during injury, which ranges from macroscale brain tissue death to nanoscale cellular organelle and biochemical changes. While it may be tempting to simply look at the macroscale tissue death as the "injury," injury actually spans across each length scale. Therefore, TBI must also be considered as a multiscale problem to identify essential brain injury mechanisms at each length scale. Specifically, consider the brain on five distinct scales: macroscale, mesoscale, microscale, nanoscale, and atomic scale, as shown in Fig. 1.1.

At the highest length scale, the macroscale is likely what individuals are most familiar with when considering the brain (and head). This scale is typically what someone will see when learning about the brain's gross anatomy. At this scale, severe injuries are typically apparent during medical imaging due to displaced tissue, tissue contusions, and hematomas, but less severe injuries that primarily affect lower length scales may be less visible. Further, damage can cause swelling, which can result in increased intracranial pressure and cause additional brain tissue damage.

The mesoscale contains the sulci and gyri geometric features of the brain's surface. These structures serve the purpose of increasing the brain's surface area, so much of the damage here will be similar to that of the macroscale. However, this complex geometry can affect the way stress waves propagate through the brain tissue and be the site of local damage resulting from macroscale deformations.

Moving down another length scale gives the microscale, which starts to be smaller than what is easily observable with the human eye. At this scale, the primary focus is how many cells are dying in a local area. Unfortunately, even if there are only a few cells killed in an initial injury, it can result in biological cascades that cause additional cells in the local area to die. This cell death happens via a combination of apoptosis (programmed cell death using ATP) and necrosis (sudden cell death that does not require ATP). with the potential for local tissue death.

At the nanoscale, changes to local cellular structures are the primary focus. This includes mechanical changes, such as mechanoporation in the membrane that can cause a loss of cell homeostasis, the activation of proteins that trigger cell death, and other direct damage to cellular structures. There are many different proteins that can be triggered here, so readers are referred to more dedicated resources for more information regarding the proteins and cascades related to these processes (Whalen et al., 2009; Farkas and Povlishock, 2007; Friedlander, 2003; Raghupathi, 2004; Wong et al., 2005).

Lastly, the atomic scale includes particle interactions, which affects the atomic interactions. Injury at this scale includes the effects of excitotoxic particles, such as calcium ions ($Ca^{2+}$).

### *1.3.2 Types of injury*

TBIs vary greatly in severity as well as the type of injury they cause, which can be largely classified as primary or secondary injury. Primary injury is manifested by localized damage in relation to a central focal point with injuries that cause direct damage, whereas secondary injury is the result of ongoing physiological response after the initial injury. Due to primary injury being a direct result of a brain insult, damage from these injuries is often observed more easily in brain imaging than secondary injury. Conversely, secondary injuries are at least partially caused by biochemical pathways and can lead to damage that exceeds the initial focal injury over a period of time (Meythaler et al., 2001) and considered by many to be the primary determinant of adverse outcomes (Farkas and Povlishock, 2007; Meythaler et al., 2001). However, secondary injury may not be as apparent in brain imaging, especially just after injury.

Diffuse axonal injury (DAI) is one form of secondary injury that can result in damage that exceeds a focal injury (Meythaler et al., 2001). DAI has been previously reported to be present in 40–50% of the TBI injuries requiring hospitalization in the United States (Meythaler et al., 2001). More importantly, it can be located in a remote location from any focal injury or lack a focal injury while being microscopic in nature, meaning that it is not easily noticed on CT and MRI imaging methods (Farkas and Povlishock, 2007; Meythaler et al., 2001). This creates a large threat that is not easily detectable despite causing damage effects throughout the brain. Axonal bulbs that result from biochemical factors will develop due to neuron damage and may result in continued myelin degeneration for years afterward (Meythaler et al., 2001). DAI has also been linked to cognitive deficits, and neurons that are affected by DAI often suffer from axon degeneration indicating membrane integrity loss (Farkas and Povlishock, 2007; Meythaler et al., 2001).

While primary and secondary injuries can both result in permanent damage to the brain through the death of neurons (Farkas and Povlishock, 2007; Raghupathi, 2004; Wong et al., 2005; Meythaler et al., 2001; DePalma et al., 2005; Maiden, 2009; Wolf et al., 2009; Shukla and Devi, 2010), injury severity will largely determine the final outcome and how long recovery will take, if possible. TBI is classified into severity categories of mild, moderate, and severe, with mild TBI often being referred to as a concussion. To determine injury severity, the Glasgow coma scale (GCS) can be used (Andriessen et al., 2010; Shukla and Devi, 2010; Haddad and Arabi, 2012). This scale is based on visual, verbal, and motor responsiveness with a higher score being indicative of less severe injury (Andriessen et al., 2010). For mild TBI, there is a loss of consciousness for less than 30 minutes, memory loss around the time of injury, and disorientation or confusion, and the GCS should be greater than 13 (Andriessen et al., 2010; Shukla and Devi, 2010). In comparison, severe TBI has a score of less than eight indicating the individual is much less responsive, which indicates greater damage. This score is a predictor of mortality risk, but it does not provide information regarding the underlying brain damage (Andriessen et al., 2010), such as if the injury was primary or secondary.

### 1.3.3 Examples of injuries

TBI events also vary greatly, with the type of event greatly influencing whether the damage will be predominantly primary or secondary in nature. Some common examples of TBI events include the head being struck by or striking an object and a projectile, such as a bullet, penetrating the skull. Pressure waves from blasts and movements without external impact that cause rapid accelerations to the head can also result in TBI (Menon et al., 2010).

Injuries sustained from the motor vehicle accident, and falls, are often due to the brain coming in contact with the inside of the skull after contact with an object and are often known as closed-head, or nonpenetrating, injuries. When this occurs, large inertial motions of the brain tissue with respect to the skull can cause brain tissue to deform excessively. These injury events can lead to both immediate primary damage and secondary damage (Pfister et al., 2003). Primary injury in this context takes the form of cerebral contusions, a form of tissue bruising where the brain contacts the skull, and secondary injury often takes the form of DAI. Depending on severity, these injuries may require immediate surgical intervention (Shukla and Devi, 2010).

Injuries sustained from skull penetration events, known as open-head or penetrating brain injury, cause a focal injury where the brain is directly damaged by an external source. This penetration can leave a cavity, cause significant primary injury, and can greatly increase the risk of detrimental effects. Further, this damage can be higher for high energy ballistics (i.e., fast-moving projectiles), which create a temporarily larger cavity through pressure waves and cause further damage, which may be increased by designs that cause a projectile to flatten or otherwise change form after entering the body (Maiden, 2009). Pressure waves resulting from these ballistics cause secondary diffuse damage that extends beyond the focal injury (Meythaler et al., 2001; Maiden, 2009).

Injuries sustained from blast waves have several factors that affect the amount of damage done by a blast, including the blast medium, the distance from the blast epicenter, and the size of the blast (Wolf et al., 2009; Moss et al., 2009). Additionally, the problem is compounded by the various types of blast injuries that occur. In a single event, a person can receive primary, secondary, tertiary, and quaternary blast injuries. Primary blast injuries are direct tissue damage from the blast overpressure, secondary blast injuries are caused by items displaced by the blast pressure wave becoming projectiles resulting in blunt force trauma or penetration, tertiary blast injuries are caused by the person being displaced by the pressure wave and injured by blunt trauma after hitting an object (e.g., a wall), and quaternary blast injuries are any injuries caused directly by the explosion but not covered by the first three injuries such as radiation, burns, or psychological trauma (Wolf et al., 2009). This assortment of injuries results in a variety of potential damages to the brain, including directly damaged tissue from skull penetrations and blast overpressure, contusions from blunt force trauma, hemorrhaging from penetration, shear damages, and possible skull flexure (Wolf et al., 2009; Moss et al., 2009; Kato et al., 2007).

Another important mode of injury that should be considered is rapid acceleration or deceleration of the head. This type of injury often occurs in conjunction with injuries when the head is exposed to a sudden acceleration change due to a force on the body (Sabet et al., 2008). For example, the above examples of motor vehicle accidents and blast injuries would both result in significant acceleration changes. Other examples would include athletes, such as fighters or football players. In many of these cases, brain injury can occur if the brain excessively deforms due to accelerations (Sabet et al., 2008). Often, this type of injury is diffuse in nature and may not have a large focal point of damage if no other type of injury occurs as well.

### *1.3.4 Neurobehavioral sequelae*

In addition to the directly observable injury, TBI often results in neurobehavioral sequeulae. A person may experience multiple neurobehavioral sequelae following an injury. These TBI sequelae can be grouped into two overarching categories: somatic and neuropsychiatric, which correspond to the physical effects and mental changes following injury (Riggio and Wong, 2009). While different in nature, both types of sequelae can be temporary or chronic in duration and can significantly impact a person's quality of life when severe, especially when chronic.

Somatic sequelae can include loss of consciousness, headache, dizziness, fatigue, sleep disturbances, and seizures as well as other effects (Riggio and Wong, 2009). While these sequelae can be acute or chronic, they often go away on their own, especially in cases of mild TBI. For example, any loss of consciousness during a mild injury typically lasts less than 30 minutes. However, some somatic sequelae, such as headaches, can last multiple months even with mild injury and can be debilitating during more severe injury (Riggio and Wong, 2009).

Neuropsychiatric sequelae include both cognitive deficits and behavioral disorders (Riggio and Wong, 2009). Cognitive deficits include impairments in attention/concentration, memory, or executive function and can interfere in performing everyday tasks or routines and a direct result of injury (Riggio and Wong, 2009; McAllister, 2011). These impairments may also affect the ability to plan or organize. Because of an inability to perform as well as before the injury, cognitive disorders may also result in depression, substance abuse, irritability, or anxiousness (Riggio and Wong, 2009; McAllister, 2011). While cognitive deficits rarely last more than 3 months, there is a correlation between loss of consciousness or post trauma amnesia and severity of the deficit (Riggio and Wong, 2009). In comparison, behavioral disorders include changes to a person's behavior postinjury, such as changes in personality, major depression, and anxiety disorders like post-traumatic stress disorder (Riggio and Wong, 2009; McAllister, 2011). These changes can be directly rooted in underlying neural damage from the injury or in cognitive problems resulting from the injury (Riggio and Wong, 2009). Changes due to physical damage to different parts of the brain can often be correlated to different behavioral disorders (McAllister, 2011). Further, fear and emotional responses brought

about by weak defense mechanisms, poor social support, or medication can be the cause of behavioral disorders (Riggio and Wong, 2009). Regardless of the cause, behavioral disorders that manifest after TBI can range in severity and be long-lasting, which can lead to significant changes to interpersonal interactions and interfere with daily life.

### 1.3.5 TBI research methods

TBI cannot be explored in a controlled setting using human subjects, so a combination of experimental and computational methods must be used. These methods cover an extremely wide range of techniques, so a very broad overview is covered here. Regardless of the method, one should keep in mind that the goal of these research methods is to elucidate the injury mechanisms and the resulting changes due to TBI. These complex interconnections, therefore, require extensive study in morphology, stress–strain response, and other biomechanical cues behind TBI.

#### 1.3.5.1 Experiments

Experiments examining injury include in vivo, ex vivo, and in vitro methods, which refer to experiments taking place inside an organism's body, outside of an organism's body after being taken from an organism, and outside a body altogether in an artificial setting. Each of these have advantages and disadvantages, including differences in the type of information they can provide.

One common in vivo method includes using animal models as representative proxies for human TBI. These models allow specific TBI aspects and outcomes can be investigated and correlated back observations in humans. For example, rats have been used with blunt impact and blast devices to study the immediate and ongoing effects of TBI (Bayly et al., 2006; Begonia et al., 2014; Shultz et al., 2017). Al studies have used rats for these studies. Examining injury in this kind of study includes a mixture of medical imaging, cell (tissue) staining, biomarkers, and observation. These observations can be made both before and following injury but can be difficult to capture during the actual injury. The primary benefits of this method are experiment repeatability in a known model, number of samples, and the ability to observe injury effects over time, including changes to behavior and biomarker concentrations. However, animal studies are limited by available resources, including equipment and laboratory space, time, and personnel, and must abide by procedural restraints as established by governing bodies. Additionally, even though there are often challenges relating common models, such as rodents, to human TBI (Agoston et al., 2019), the cost and related restrictions increase dramatically when using larger animal models or nonhuman primates.

Another in vivo method includes medically imaging, observing human subjects postinjury, and postmortem findings. This has led to many discoveries related to TBI, but each injury is unique (i.e., not controlled) and observations are limited to only postinjury in most

cases, meaning they lack a preinjury state for comparison. One exception to this are studies that include individuals participating in activities with a high-risk of TBI. In these cases, an individual's brain can be scanned prior to injury to create an individualized brain model (Garimella et al., 2019). By wearing sensors that detect potential injury events (e.g., impacts or blasts), these boundary conditions can be used to generate individualized simulations (Garimella et al., 2019). If necessary, the person in question could also be rescanned following injury to confirm whether injury has occurred and to what severity.

Ex vivo experiments include mechanical testing of tissues removed from the body. Because brain tissue has rate-dependent (Arbogast et al., 1995; Begonia et al., 2010; Prabhu et al., 2019) and anisotropic (Arbogast and Margulies, 1997) mechanical properties, both high- and low-rate and different stress state testing are needed. For low-rate testing, micromechanical devices are used for testing (Begonia et al., 2010; Prabhu et al., 2019). Note that the load cells with these devices must be matched with the material being tested, so a load cell of ~1 kg is often used with for brain tissue (Begonia et al., 2010; Prabhu et al., 2019). For high-rate testing, the split Hopkinson pressure bar is more appropriate (Prabhu et al., 2019; Pervin and Chen, 2009). Rather than measuring load directly with a load cell as typically used for low-rate devices, split Hopkinson pressure bar measure the change in pressure along the bars using strain gauges. Therefore, the bar material is important because an overly stiff bar will not be sensitive enough to identify deforming soft materials compared to changes in the bar. While traditional bars are made of steel for testing metals, softer bars with lower impedance, such as hollow aluminum (Pervin and Chen, 2009) and polycarbonate (Prabhu et al., 2019), are used for soft materials to better match impedance between bar and material. While these mechanical experiments provide a better understanding of tissue properties, testing is often destructive to the sample, especially during high-rate testing. Hence, they require interruption-testing (stopping a test mid-way) to investigate intermediate deformation states. Additionally, these tests do not provide any insight into ongoing injury effects as occurs in the body, such as biomarkers.

In vitro experiments differ from in vivo and ex vivo in that the samples are completely maintained outside the body, such as cell cultures (Geddes et al., 2003; Farkas et al., 2006; Kilinc et al., 2008). For example, in vitro cell culture experiments have shown that membrane mechanoporation results in membrane disruptions and increases membrane permeability postinjury (Geddes et al., 2003; Farkas et al., 2006; Kilinc et al., 2008), which can cause a loss of cell homeostasis. While many of these culture studies are performed on a single plane, some researchers have implemented 3D cell culture to better replicate their natural structure (LaPlaca and Thibault, 1997; Cullen et al., 2007, 2011). Many properties, such as physiological changes, mechanical properties, or fluorescence expression, can be examined using cultures and should be chosen as appropriate for each problem. However, the difference between local forces and macroscale forces as well as culture neuron heterogeneities, orientation, and processes in comparison to natural tissue must be considered when performing mechanical tests (Cullen and LaPlaca, 2006).

One final branch of experiments is TBI equipment efficacy testing. These experiments differ from the others mentioned here in that they often do not include a biological component. Rather, they use a testing apparatus with a helmeted headform, such as a drop tower (NOCSAE, 2019; Rush et al., 2017; Bliven et al., 2019). This type of experiment allows for equipment to be tested for minimum safety requirements and graded based on standardized rubrics.

#### 1.3.5.2 Computational models (simulations)

While experiments help to identify potential injury locations of interest, they can be complemented by in silico computational methods. Researchers have developed computational models at different length scales to develop a more comprehensive picture of TBI and establish brain injury thresholds (Prabhu et al., 2011; Murphy et al., 2016, 2018; Alaei, 2017; Montanino, 2019; Rashid et al., 2013, 2014; Bakhtiarydavijani et al., 2019b, 2019a). Multiscale in silico models help to investigate potential injury mechanisms across length and time scales, which ultimately serve as a noninvasive predictor in primary responses to TBI (Montanino, 2019; Bakhtiarydavijani et al., 2019b, 2019a). Additionally, models have the benefit of no ongoing consumable costs as seen in many experiments and may require less personnel to run. However, initial model development and software licenses can be expensive upfront costs.

As shown in Fig. 1.1, each length scale has both information it needs and what information it can provide—similarly, computational models are limited in what they can include. Unlike real-world experiments, which inherently include information on lower-length scales, even though it may not be easily accessed, many computational models only include details for the scale being examined. In this case, any information needed from other length scales must be passed into the model through boundary conditions, material models, or some other method.

Take, for example, finite element analysis (FEA), which is often used to examine TBI. Because FEA is a continuum method, FEA simulations require constitutive material models to better replicate the brain's morphology for more accurate stress responses that general material models do not capture (Prabhu et al., 2011; Cloots et al., 2008; Yang et al., 2014; Colgan et al., 2010). Specifically, the constitutive material models better capture effects from lower length scale changes and related changes to the brain. Without these details, the model cannot capture history effects and dependencies on rate and stress state. Similarly, a constitutive model is required for injury effects to be implemented, which some studies have done through damage criteria (El Sayed et al., 2008; Prevost et al., 2011; McElhaney et al., 1973; Mihai et al., 2017; de Rooij and Kuhl, 2018; Weickenmeier et al., 2017). However, a true rubric based on changes to the lower length scales is needed.

Due to small length and time scales making it difficult to experimentally capture sufficient information for lower length scale injury effects, lower-length scale simulations must be considered. For example, molecular dynamics can be used to explore the mechanical properties

of the cellular membrane structure and deformation-related mechanoporation damage (Murphy et al., 2016, 2018; Koshiyama and Wada, 2011; Shigematsu et al., 2014, 2015). In addition to providing a better understanding of cell membrane mechanoporation, results from the simulations can be used to estimate cell ion permeation (Bakhtiarydavijani et al., 2019a). Creating a more robust model of TBI with these underlying details will aid in determining cellular death and injury.

This brief description is intended to provide a general description of the multiscale modeling process. More detailed descriptions of methods used at each length scale will be covered in the chapters included herein.

## 1.4 Summary

The human brain is a complex multiscale system comprised of several elements, which are highly interconnected in a structural hierarchy and concurrently work at different levels of organization (Bastiani and Roebroeck, 2015; van den Heuvel and Yeo, 2017). From the macroscale brain cortical structures to the microscale cellular structures and the nanoscale cellular components, the brain's length scales span nine orders of magnitude, each with a distinct organization. Is it any wonder then that TBI is also complex in its mechanisms and effects? A result of direct impacts and accelerations to the head, TBI causes a combination of focal and diffuse injuries that lead to cell death in the brain and a variety of injury sequelae that can be debilitating when severe or chronic. Due to the severity and frequency of TBI, a variety of methods must be considered to study the mechanisms behind the injury. While real-world observations of TBI and experiments can provide many insights into injury, computer models can help elucidate TBI mechanisms that cannot be readily observed.

## References

Aggleton, J.P., O'Mara, S.M., Vann, S.D., Wright, N.F., Tsanov, M., Erichsen, J.T., 2010. Hippocampal-anterior thalamic pathways for memory: uncovering a network of direct and indirect actions. Eur. J. Neurosci. 31, 2292–2307. https://doi.org/10.1111/j.1460-9568.2010.07251.x.

Agoston, D.V., Vink, R., Helmy, A., Risling, M., Nelson, D., Prins, M., 2019. How to translate time: the temporal aspects of rodent and human pathobiological processes in traumatic brain injury. J. Neurotrauma 36, 1724–1737. https://doi.org/10.1089/neu.2018.6261.

Alaei, Z., 2017. Molecular dynamics simulations of axonal membrane in traumatic brain injury. Master thesis, KTH Royal Institute of Technology, School of Technology and Health (STH), Stockholm, Sweden. https://kth.diva-portal.org/smash/get/diva2:1127564/FULLTEXT01.pdf.

Alberts, B., Johnson, A., Lewis, J., Morgan, D., Raff, M., Roberts, K., et al., 2014. Molecular Biology of the Cell. W. W. Norton & Company, New York, NY.

Andriessen, T., Jacobs, B., Vos, P.E., 2010. Clinical characteristics and pathophysiological mechanisms of focal and diffuse traumatic brain injury. J. Cell. Mol. Med. 14, 2381–2392. https://doi.org/10.1111/j.1582-4934.2010.01164.x.

Arbogast, K.B., Margulies, S.S., 1997. Regional Differences in Mechanical Properties of the Porcine Central Nervous System. 41st Stapp Car Crash Conference 106, 3807–3814. https://doi.org/10.4271/973336.

Arbogast, K.B., Meaney, D.F., Thibault, L.E., 1995. Biomechanical Characterization of the Constitutive Relationship for the Brainstem. SAE International. https://doi.org/10.4271/952716.
Aulinas, A., 2000. Physiology of the Pineal Gland and Melatonin. MDText.com, Inc, South Dartmouth, MA.
Azevedo, F.A.C., Carvalho, L.R.B., Grinberg, L.T., Farfel, J.M., Ferretti, R.E.L., Leite, R.E.P., et al., 2009. Equal numbers of neuronal and nonneuronal cells make the human brain an isometrically scaled-up primate brain. J. Comp. Neurol. 513, 532–541. https://doi.org/10.1002/cne.21974.
Bakhtiarydavijani, A., Murphy, M.A., Mun, S., Jones, M.D., Bammann, D.J., LaPlaca, M.C., et al., 2019a. Damage biomechanics for neuronal membrane mechanoporation. Model Simul. Mater. Sci. Eng. 27, 065004. https://doi.org/10.1088/1361-651X/ab1efe.
Bakhtiarydavijani, A.H., Murphy, M.A., Mun, S., Jones, M.D., Horstemeyer, M.F., Prabhu, R.K., 2019b. Multiscale modeling of the damage biomechanics of traumatic brain injury. Biophys. J. 116, 322a. https://doi.org/10.1016/j.bpj.2018.11.1748.
Bastiani, M., Roebroeck, A., 2015. Unraveling the multiscale structural organization and connectivity of the human brain: the role of diffusion MRI. Front. Neuroanat 9, 77. https://doi.org/10.3389/fnana.2015.00077.
Bayly, P.V., Black, E.E., Pedersen, R.C., Leister, E.P., Genin, G.M., 2006. In vivo imaging of rapid deformation and strain in an animal model of traumatic brain injury. J. Biomech. 39, 1086–1095. https://doi.org/10.1016/j.jbiomech.2005.02.014.
Begonia, M.T., Prabhu, R., Liao, J., Horstemeyer, M.F., Williams, L.N., 2010. The influence of strain rate dependency on the structure–property relations of porcine brain. Ann. Biomed. Eng. 38, 3043–3057. https://doi.org/10.1007/s10439-010-0072-9.
Begonia, M.T., Prabhu, R., Liao, J., Whittington, W.R., Claude, A., Willeford, B., et al., 2014. Quantitative analysis of brain microstructure following mild blunt and blast trauma. J. Biomech. 47, 3704–3711. https://doi.org/10.1016/j.jbiomech.2014.09.026.
Bigos, K., Hariri, A., Weinberger, D., 2016. Neuroimaging Genetics: Principles and Practices. Oxford University Press, Oxford, UK.
Bliven, E., Rouhier, A., Tsai, S., Willinger, R., Bourdet, N., Deck, C., et al., 2019. Evaluation of a novel bicycle helmet concept in oblique impact testing. Accid. Anal. Prev. 124, 58–65. https://doi.org/10.1016/j.aap.2018.12.017.
Boron, W.F., Boulpaep, E.L., 2016. Medical Physiology. Elsevier, Philadelphia, PA. https://doi.org/10.1016/s0033-3182(64)72477-2.
Caputo, A., Ghiringhelli, L., Dieci, M., Giobbio, G.M., Tenconi, F., Ferrari, L., et al., 1998. Epithalamus calcifications in schizophrenia. Eur. Arch. Psychiatry Clin. Neurosci. 248, 272–276. https://doi.org/10.1007/s004060050049.
Catani, M., Dell'Acqua, F., De Schotten, M.T., 2013. A revised limbic system model for memory, emotion and behaviour. Neurosci. Biobehav. Rev. 37 (8), 1724–1737. https://doi.org/10.1016/j.neubiorev.2013.07.001.
Cloots, R.J.H., Gervaise, H.M.T., van Dommelen, J.A.W., Geers, M.G.D., 2008. Biomechanics of traumatic brain injury: influences of the morphologic heterogeneities of the cerebral cortex. Ann. Biomed. Eng. 36, 1203–1215. https://doi.org/10.1007/s10439-008-9510-3.
Colgan, N.C., Gilchrist, M.D., Curran, K.M., 2010. Applying DTI white matter orientations to finite element head models to examine diffuse TBI under high rotational accelerations. Prog. Biophys. Mol. Biol. 103, 304–309. https://doi.org/10.1016/j.pbiomolbio.2010.09.008.
Cullen, D.K., LaPlaca, M.C., 2006. Neuronal response to high rate shear deformation depends on heterogeneity of the local strain field. J. Neurotrauma 23, 1304–1319. https://doi.org/10.1089/neu.2006.23.1304.
Cullen, D.K., Simon, C.M., LaPlaca, M.C., 2007. Strain rate-dependent induction of reactive astrogliosis and cell death in three-dimensional neuronal–astrocytic co-cultures. Brain Res. 1158, 103–115. https://doi.org/10.1016/j.brainres.2007.04.070.
Cullen, D.K., Vernekar, V.N., LaPlaca, M.C., 2011. Trauma-induced plasmalemma disruptions in three-dimensional neural cultures are dependent on strain modality and rate. J. Neurotrauma 28, 2219–2233. https://doi.org/10.1089/neu.2011.1841.
Davey, G., 2011. Applied Psychology. Wiley, Hoboken, NJ.

de Rooij, R., Kuhl, E., 2018. A physical multifield model predicts the development of volume and structure in the human brain. J. Mech. Phys. Solids 112, 563–576. https://doi.org/10.1016/j.jmps.2017.12.011.

Decimo, I., Fumagalli, G., Berton, V., Krampera, M., Bifari, F., 2012. Meninges: from protective membrane to stem cell niche. Am. J. Stem Cells 1, 92–105.

DePalma, R.G., Burris, D.G., Champion, H.R., Hodgson, M.J., 2005. Blast Injuries. N. Engl. J. Med. 352, 1335–1342. https://doi.org/10.1056/NEJMra042083.

El Sayed, T., Mota, A., Fraternali, F., Ortiz, M., 2008. A variational constitutive model for soft biological tissues. J. Biomech. 41, 1458–1466. https://doi.org/10.1016/j.jbiomech.2008.02.023.

Farkas, O., Lifshitz, J., Povlishock, J.T., 2006. Mechanoporation induced by diffuse traumatic brain injury: an irreversible or reversible response to injury? J. Neurosci. 26, 3130–3140. https://doi.org/10.1523/JNEUROSCI.5119-05.2006.

Farkas, O., Povlishock, J.T., 2007. Cellular and subcellular change evoked by diffuse traumatic brain injury: a complex web of change extending far beyond focal damage. In: Weber, J.T., Maas, A.I.R. (Eds.). Progress in Brain Research, 161. Elsevier, Amsterdam; Boston, pp. 43–59. https://doi.org/10.1016/S0079-6123(06)61004-2.

Fine, E.J., Ionita, C.C., Lohr, L., 2002. The history of the development of the cerebellar examination. Semin. Neurol. 22, 375–384. https://doi.org/10.1055/s-2002-36759.

Fletcher, D.A., Mullins, R.D., 2010. Cell mechanics and the cytoskeleton. Nature 463, 485–492. https://doi.org/10.1038/nature08908.

Freberg, L., 2009. Discovering Biological Psychology. Cengage Learning, Boston, MA.

Friedlander, R.M., 2003. Apoptosis and caspases in neurodegenerative diseases. N. Engl. J. Med. 348, 1365–1375. https://doi.org/10.1056/NEJMra022366.

Garimella, H.T., Menghani, R.R., Gerber, J.I., Sridhar, S., Kraft, R.H., 2019. Embedded finite elements for modeling axonal injury. Ann. Biomed. Eng. 47, 1889–1907. https://doi.org/10.1007/s10439-018-02166-0.

Gazzaniga, M.S., Ivry, R.B., Mangun, G.R., 2014. Cognitive Neuroscience - The Biology of The Mind. New York: W. W. Norton.

Geddes, D.M., Cargill 2nd, R.S., LaPlaca, M.C., 2003. Mechanical stretch to neurons results in a strain rate and magnitude-dependent increase in plasma membrane permeability. J. Neurotrauma 20, 1039–1049. https://doi.org/10.1089/089771503770195885.

Ginhoux, F., Lim, S., Hoeffel, G., Low, D., Huber, T., 2013. Origin and differentiation of microglia. Front. Cell Neurosci. 7, 1–14. https://doi.org/10.3389/fncel.2013.00045.

Giordano, C., Kleiven, S., 2014. Evaluation of axonal strain as a predictor for mild traumatic brain injuries using finite element modeling. Stapp Car Crash 58, 29–61.

Gray, H., Standring, S., 2015. Gray's Anatomy: The Anatomical Basis of Clinical Practice. Elsevier Health Sciences, New York, NY.

Guyton, A.C., Hall, J.E., 2011. Guyton and Hall Textbook of Medical Physiology, 12th ed. Saunders, Philadelphia, PA.

Haddad, S.H., Arabi, Y.M., 2012. Critical care management of severe traumatic brain injury in adults. Scand. J. Trauma Resusc. Emerg. Med. 20, 12. https://doi.org/10.1186/1757-7241-20-12.

Harayama, T., Riezman, H., 2018. Understanding the diversity of membrane lipid composition. Nat. Rev. Mol. Cell. Biol. 19, 281–296. https://doi.org/10.1038/nrm.2017.138.

Harvey, A.K., Thompson, M.S., Cochlin, L.E., Raju, P.A., Cui, Z., Cornell, H.R., et al., 2009. Functional imaging of tendon. Ann. BMVA 2009, 1–11.

Helmut, K., Hanisch, U.K., Noda, M., Verkhratsky, A., 2011. Physiology of microglia. Physiol. Rev. 91, 461–553. https://doi.org/10.1152/physrev.00011.2010.

Herculano-Houzel, S., 2014. The glia/neuron ratio: how it varies uniformly across brain structures and species and what that means for brain physiology and evolution. Glia 62, 1377–1391. https://doi.org/10.1002/glia.22683.

Higgins, V., 2006. Human physiology: the basis of medicine. Oxford University Press, Oxford, UK.

Humphreys, I., Wood, R.L., Phillips, C.J., Macey, S., 2013. The costs of traumatic brain injury: a literature review. Clinicoecon. Outcomes Res. 5, 281–287. https://doi.org/10.2147/CEOR.S44625.

Johnson, V.E., Stewart, W., Smith, D.H., 2013. Axonal pathology in traumatic brain injury. Exp. Neurol. 246, 35–43. https://doi.org/10.1016/j.expneurol.2012.01.013.

Kandel, E., Schwartz, J., Jessell, T., 2000. Principles of neural science. McGraw-hill, New York.
Kato, K., Fujimura, M., Nakagawa, A., Saito, A., Ohki, T., Takayama, K., et al., 2007. Pressure-dependent effect of shock waves on rat brain: induction of neuronal apoptosis mediated by a caspase-dependent pathway. J. Neurosurg. 106, 667–676. https://doi.org/10.3171/jns.2007.106.4.667.
Kekere, V., Alsayouri, K., 2019. Anatomy, Head and Neck, Dura Mater. StatPearls, Treasure Island, FL.
Kilinc, D., Gallo, G., Barbee, K.A., 2008. Mechanically-induced membrane poration causes axonal beading and localized cytoskeletal damage. Exp. Neurol. 212, 422–430. https://doi.org/10.1016/j.expneurol.2008.04.025.
Kolb, B., Whishaw, I.Q., 2009. Fundamentals of Human Neuropsychology. Macmillan, New York, NY.
Kole, M.H.P., Ilschner, S.U., Kampa, B.M., Williams, S.R., Ruben, P.C., Stuart, G.J., 2008. Action potential generation requires a high sodium channel density in the axon initial segment. Nature 11, 178–186. https://doi.org/10.1038/nn2040.
Koshiyama, K., Wada, S., 2011. Molecular dynamics simulations of pore formation dynamics during the rupture process of a phospholipid bilayer caused by high-speed equibiaxial stretching. J. Biomech. 44, 2053–2058. https://doi.org/10.1016/j.jbiomech.2011.05.014.
LaPlaca, M., Thibault, L., 1997. An in vitro traumatic injury model to examine the response of neurons to a hydrodynamically-induced deformation. Ann. Biomed. Eng. 25, 665–677. https://doi.org/10.1007/BF02684844.
Leterrier, C., Dubey, P., Roy, S., 2017. The nano-architecture of the axonal cytoskeleton. Nat. Rev. Neurosci. 18, 713–726. https://doi.org/10.1038/nrn.2017.129.
Lowrey, P.L., Takahashi, J.S., 2000. Genetics of the mammalian circadian system: photic entrainment, circadian pacemaker mechanisms, and posttranslational regulation. Annu. Rev. Genet. 34, 533–562. https://doi.org/10.1146/annurev.genet.34.1.533.
Maiden, N., 2009. Ballistics reviews: mechanisms of bullet wound trauma. Forensic Sci. Med. Pathol. 5, 204–209. https://doi.org/10.1007/s12024-009-9096-6.
McAllister, T.W., 2011. Neurobiological consequenses of traumatic brain injury. Dialog. Clin. Neurosci. 13, 287–300.
McElhaney, J.H., Melvin, J.W., Roberts, V.L., Portnoy, H.D., 1973. Dynamic Characteristics of the Tissue of the Head. Palgrave Macmillan, London, 215–222.
Menon, D.K., Schwab, K., Wright, D.W., Maas, A.I., 2010. Position statement: definition of traumatic brain injury. Arch. Phys. Med. Rehabil. 91, 1637–1640.
Meythaler, J.M., Peduzzi, J.D., Eleftheriou, E., Novack, T.A., 2001. Current concepts: diffuse axonal injury-associated traumatic brain injury. Arch. Phys. Med. Rehabil. 82, 1461–1471.
Mihai, L.A., Budday, S., Holzapfel, G.A., Kuhl, E., Goriely, A., 2017. A family of hyperelastic models for human brain tissue. J. Mech. Phys. Solids 106, 60–79. https://doi.org/10.1016/j.jmps.2017.05.015.
Montanino, A., 2019. Definition of Axonal Injury Tolerances Across Scales. PhD Thesis, KTH Royal Institute of Technology, Stockholm, Sweden. http://kth.diva-portal.org/smash/get/diva2:1387578/FULLTEXT01.pdf.
Moss, W.C., King, M.J., Blackman, E.G., 2009. Skull flexure from blast waves: a mechanism for brain injury with implications for helmet design. Phys. Rev. Lett. 103, 108702.
Murphy, M.A., Horstemeyer, M.F.F., Gwaltney, S.R., Stone, T., Laplaca, M.C., Liao, J., et al., 2016. Nanomechanics of phospholipid bilayer failure under strip biaxial stretching using molecular dynamics. Model Simul. Mater. Sci. Eng. 24, 055008. https://doi.org/10.1088/0965-0393/24/5/055008.
Murphy, M.A., Mun, S., Horstemeyer, M.F., Baskes, M.I., Bakhtiary, A., LaPlaca, M.C., et al., 2018. Molecular dynamics simulations showing 1-palmitoyl-2-oleoyl-phosphatidylcholine (POPC) membrane mechanoporation damage under different strain paths. J. Biomol. Struct. Dyn. 37, 1–14. https://doi.org/10.1080/07391102.2018.1453376.
NOCSAE. Standard Performance Specification For Newly Manufactured Football Helmets NOCSAE DOC (ND)002-17m19. National Operating Committee on Standards For Athletic Equipment. 2019. https://doi.org/NOCSAEDOC(ND)002-17m19.
Oberheim, N.A., Goldman, S.A., Nedergaard, M., 2012. Heterogeneity of astrocytic form and function. Methods Mol. Biol. 814, 23–45. https://doi.org/10.1007/978-1-61779-452-0_3.

Patel, N., Kirmi, O., 2009. Anatomy and imaging of the normal meninges. Semin. Ultrasound CT MRI 30, 559–564. https://doi.org/10.1053/j.sult.2009.08.006.

Patestas, M., Gartner, L., 2016. A Textbook of Neuroanatomy. Wiley, Hoboken, NJ.

Pervin, F., Chen, W.W., 2009. Dynamic mechanical response of bovine gray matter and white matter brain tissues under compression. J. Biomech. 42, 731–735. https://doi.org/10.1016/j.jbiomech.2009.01.023.

Pfister, B.J., Weihs, T.P., Betenbaugh, M., Bao, G., 2003. An in vitro uniaxial stretch model for axonal injury. Ann. Biomed. Eng. 31, 589–598. https://doi.org/10.1114/1.1566445.

Prabhu, R., Horstemeyer, M.F., Tucker, M.T., Marin, E.B., Bouvard, J.L., Sherburn, J.A., et al., 2011. Coupled experiment/finite element analysis on the mechanical response of porcine brain under high strain rates. J. Mech. Behav. Biomed. Mater. 4, 1067–1080. https://doi.org/10.1016/j.jmbbm.2011.03.015.

Prabhu, R.K., Begonia, M.T., Whittington, W.R., Murphy, M.A., Mao, Y., Liao, J., et al., 2019. Compressive mechanical properties of porcine brain: experimentation and modeling of the tissue hydration effects. Bioengineering 6, 40. https://doi.org/10.3390/bioengineering6020040.

Prevost, T.P., Balakrishnan, A., Suresh, S., Socrate, S., 2011. Biomechanics of brain tissue. Acta Biomater. 7, 83–95. https://doi.org/10.1016/j.actbio.2010.06.035.

Purves, D., 2012. Neuroscience, fifth ed. Sinauer Associates Inc, Sunderland, MA.

Raghupathi, R., 2004. Cell death mechanisms following traumatic brain injury. Brain Pathol. 14, 215–222. https://doi.org/10.1111/j.1750-3639.2004.tb00056.x.

Rashid, B., Destrade, M., Gilchrist, M.D., 2013. Mechanical characterization of brain tissue in simple shear at dynamic strain rates. J. Mech. Behav. Biomed. Mater. 28, 71–85. https://doi.org/10.1016/j.jmbbm.2013.07.017.

Rashid, B., Destrade, M., Gilchrist, M.D., 2014. Mechanical characterization of brain tissue in tension at dynamic strain rates. Forensic Biomech. 33, 43–54. https://doi.org/10.1016/j.jmbbm.2012.07.015.

Riggio, S., Wong, M., 2009. Neurobehavioral sequelae of traumatic brain injury. Mt Sinai J. Med. A J. Transl. Pers. Med. 76, 163–172. https://doi.org/10.1002/msj.20097.

Rush, G.A., Rush, G.A., Sbravati, N., Prabhu, R., Williams, L.N., DuBien, J.L., et al., 2017. Comparison of shell-facemask responses in American football helmets during NOCSAE drop tests. Sport Eng. 20, 199–211. https://doi.org/10.1007/s12283-017-0233-2.

Saab, A.S., Nave, K.A., 2017. Myelin dynamics: protecting and shaping neuronal functions. Curr. Opin. Neurobiol. 47, 104–112. https://doi.org/10.1016/j.conb.2017.09.013.

Sabet, A.A., Christoforou, E., Zatlin, B., Genin, G.M., Bayly, P.V., 2008. Deformation of the human brain induced by mild angular head acceleration. J. Biomech. 41, 307–315. https://doi.org/10.1016/j.jbiomech.2007.09.016.

Sampaio-Baptista, C., Johansen-Berg, H., 2017. White matter plasticity in the adult brain. Neuron 96, 1239–1251. https://doi.org/10.1016/j.neuron.2017.11.026.

Sherman, S., 2006. Thalamus. Scholarpedia 1, 1583. https://doi.org/10.4249/scholarpedia.1583.

Sherman, S.M., Guillery, R.W., 2009. Exploring the Thalamus and Its Role in Cortical Function. The MIT Press, Cambridge, MA.

Shigematsu, T., Koshiyama, K., Wada, S., 2014. Molecular dynamics simulations of pore formation in stretched phospholipid/cholesterol bilayers. Chem. Phys. Lipids 183, 43–49. https://doi.org/10.1016/j.chemphyslip.2014.05.005.

Shigematsu, T., Koshiyama, K., Wada, S., 2015. Effects of stretching speed on mechanical rupture of phospholipid/cholesterol bilayers: molecular dynamics simulation. Sci. Rep. 5, 15369. https://doi.org/10.1038/srep15369.

Shukla, D., Devi, B.I., 2010. Mild traumatic brain injuries in adults. J. Neurosci. Rural Prac.t 01, 082–088. https://doi.org/10.4103/0976-3147.71723.

Shultz, S.R., McDonald, S.J., Vonder Haar, C., Meconi, A., Vink, R., van Donkelaar, P., et al., 2017. The potential for animal models to provide insight into mild traumatic brain injury: translational challenges and strategies. Neurosci. Biobehav. Rev. 76, 396–414. https://doi.org/10.1016/j.neubiorev.2016.09.014.

Snell, R.S., 2010. Clinical Neuroanatomy. Lippincott Williams & Wilkins, Philadelphia, PA.

Squire, L.R., Berg, D., Bloom, F.E., Du Lac, S., Ghosh, A., Spitzer, N.C., 2013. Fundamental Neuroscience. Elsevier, Cambridge, MA. https://doi.org/10.1016/C2010-0-65035-8.

Stocco, A., Lebiere, C., Anderson, J.R., 2010. Conditional routing of information to the cortex: a model of the basal ganglia's role in cognitive coordination. Psychol. Rev. 117, 541–574. https://doi.org/10.1037/a0019077.

Taylor, C.A., Bell, J.M., Breiding, M.J., Xu, L., 2017. Traumatic brain injury-related emergency department visits, hospitalizations, and deaths -- United States, 2007 and 2013. MMWR Surveill. Summ. 66, 1–16. https://doi.org/10.15585/mmwr.ss6609a1.

Teeter, C.M., Stevens, C.F., 2011. A general principle of neural arbor branch density. Curr. Biol. 21, 2105–2108. https://doi.org/10.1016/j.cub.2011.11.013.

van den Heuvel, M.P., Yeo, B.T.T., 2017. A spotlight on bridging microscale and macroscale human brain architecture. Neuron 93, 1248–1251. https://doi.org/10.1016/j.neuron.2017.02.048.

Weickenmeier, J., Saez, P., Butler, C.A.M., Young, P.G., Goriely, A., Kuhl, E., 2017. Bulging brains. J. Elast. 129, 197–212. https://doi.org/10.1007/s10659-016-9606-1.

Whalen, M.J., Yager, P., Lo, E.H., Lok, J., Noviski, N., 2009. XXXXX. In: Wheeler, D.S., Wong, H.R., Shanley, T.P. (Eds.), Molecular Biology of Brain Injury: The Central Nervous System in Pediatric Critical Illness and Injury. Springer, London, pp. 1–12. https://doi.org/10.1007/978-1-84800-993-6_2.

Wolf, S.J., Bebarta, V.S., Bonnett, C.J., Pons, P.T., Cantrill, S.V., 2009. Blast injuries. Lancet 374, 405–415. https://doi.org/10.1016/s0140-6736(09)60257-9.

Wong, J., Hoe, N., Zhiwei, F., Ng, I., 2005. Apoptosis and traumatic brain injury. Neurocrit. Care 3, 177–182. https://doi.org/10.1385/ncc:3:2:177.

Yang, B., Tse, K.-.M., Chen, N., Tan, L.-.B., Zheng, Q.-.Q., Yang, H.-.M., et al., 2014. Development of a finite element head model for the study of impact head injury. Biomed. Res. Int. 2014, 1–14. https://doi.org/10.1155/2014/408278.